THE JOURNAL OF BIOLOGICAL CHEMISTRY VOL. 287, NO. 12, pp. 9346–9359, March 16, 2012

EphA Signaling Promotes Actin-based Dendritic Spine Remodeling through Slingshot Phosphatase*[S]

Received for publication, September 9, 2011, and in revised form, January 23, 2012 Published, JBC Papers in Press, January 26, 2012, DOI 10.1074/jbc.M111.302802

Lei Zhou[1,2], **Emma V. Jones**[2], **and Keith K. Murai**[3]

From the Centre for Research in Neuroscience, Department of Neurology and Neurosurgery, The Research Institute of the McGill University Health Centre, Montreal General Hospital, Montreal, Quebec H3G 1A4, Canada

Background: The actin cytoskeleton regulates the structure of synapses formed on dendritic spines in the brain.
Results: EphA receptors modify actin and spine architecture through cofilin and the phosphatases Slingshot 1 and calcineurin/PP2B.
Conclusion: EphA receptors promote cofilin activation to induce actin remodeling in spines.
Significance: Complex signaling events involving EphA receptors control structural plasticity of brain connections.

Actin cytoskeletal remodeling plays a critical role in transforming the morphology of subcellular structures across various cell types. In the brain, restructuring of dendritic spines through actin cytoskeleletal reorganization is implicated in the regulation of synaptic efficacy and the storage of information in neural circuits. However, the upstream pathways that provoke actin-based spine changes remain only partly understood. Here we show that EphA receptor signaling remodels spines by triggering a sequence of events involving actin filament rearrangement and synapse/spine reorganization. Rapid EphA signaling over minutes activates the actin filament depolymerizing/severing factor cofilin, alters F-actin distribution in spines, and causes transient spine elongation through the phosphatases slingshot 1 (SSH1) and calcineurin/protein phosphatase 2B (PP2B). This early phase of spine extension is followed by synaptic reorganization events that take place over minutes to hours and involve the relocation of pre/postsynaptic components and ultimately spine retraction. Thus, EphA receptors utilize discrete cellular and molecular pathways to promote actin-based structural plasticity of excitatory synapses.

The refinement of neural circuits through synaptic remodeling and turnover is believed to play a critical role in brain plasticity (1, 2). Indeed, adjusting the balance of synapse assembly and disassembly in the developing and adult brain is implicated in learning and memory processes (3–7). Disruption of this balance occurs in degenerative diseases (8) and neuropsychiatric disorders (9) and underscores the importance of identifying mechanisms involved in coordinating synaptic changes.

The remodeling of dendritic spines, in particular, is believed to underlie cognitive processes in the brain (1). Spines are the main site of excitatory synapses and vary in morphology and size. They typically have an enlarged head that is connected to the dendrite shaft by a constricted neck. This architecture helps compartmentalize ion channels, scaffolding proteins, and other signaling components at postsynaptic sites (10). Single spine analysis has shown that they exhibit activity-dependent structural changes, which are believed to help establish and maintain synaptic efficacy (11–13). Intriguingly, spine number and turnover can be regulated *in vivo* by behavioral training (5, 6, 14). Thus, reconfiguring the properties of spines is an important feature of neurons and likely required for the storage of information at synapses.

A complex network of signaling pathways impinge upon the actin cytoskeletal framework of spines to govern their structural dynamics and molecular composition (15, 16). Several pools of actin are enriched in spines and in a constant state of dynamic equilibrium between filamentous (F-actin) and globular (G-actin) forms (17, 18). This equilibrium is readjusted by synaptic activity (11, 19) and the recruitment of molecules that fine-tune the complexity of the actin network (16, 20). Interestingly, increases and decreases in actin polymerization and spine size occur with long term potentiation (LTP)[4] and long term depression, respectively (11), two forms of synaptic plasticity implicated in the storage of information in neural connections. Stabilizing actin filaments or inhibiting actin polymerization blocks spine dynamics and prevents the induction and maintenance of LTP in hippocampal slices (19, 21). Thus, reorganization of the actin cytoskeleton is important for spine remodeling and associated changes in synaptic strength.

The actin cytoskeleton in neurons is organized through a multitude of pathways including those downstream of Rho GTPases, Arp2/3, and other molecules (16). Several proteins in these signaling pathways have robust effects on the morphogenesis and maintenance of spines. Among these proteins, cofilin/ADF (actin-depolymerization factor) family proteins bind, depolymerize, and sever actin filaments (22) and play an important role in spine remodeling (23–26). The activity of cofilin is

* This work was supported by the Canadian Institutes of Health Research, the Canada Research Chairs Program, the Canadian Foundation for Innovation, and the EJLB Foundation (to K. K. M.).
[S] This article contains supplemental Figs. S1 and S2.
[1] Supported by a studentship from Research Institute of the McGill University Health Centre.
[2] Both authors contributed equally to this work.
[3] To whom correspondence should be addressed: Centre for Research in Neuroscience, 1650 Cedar Ave. L7-212, Montreal, QC H3G 1A4, Canada. Tel.: 514-934-1934, Ext. 43477; Fax: 514-934-8216; E-mail: keith.murai@mcgill.ca.

[4] The abbreviations used are: LTP, long term potentiation; SFV, Semliki Forest virus; EGFP-f, farnesylated enhanced green fluorescent protein; DIV, days *in vitro*; ANOVA, analysis of variance.

directly regulated by phosphorylation/dephosphorylation events. Phosphorylation of serine 3 of cofilin by Lim kinases (LimKs) and Tes kinases inactivates cofilin, whereas dephosphorylation by Slingshot and chronophin reactivates it (27). Cofilin phosphorylation by LimK1 has been implicated in spine growth and LTP (28, 29), whereas dephosphorylation is linked to spine shrinkage and long term depression (24). Temporal regulation of cofilin phosphorylation also plays a critical role in glutamate receptor trafficking during LTP (30). Thus, cofilin is an integral component of cytoskeletal remodeling in spines and synaptic regulation. However, the upstream receptors and signaling proteins that recruit cofilin and coordinate its ability to stabilize/destabilize F-actin in spines remain poorly understood.

Eph receptors are one class of proteins that trigger changes in spine morphology (31–33). Eph receptors comprise a family of receptor tyrosine kinases that are activated by ligands known as ephrins. In general, ephrin-As and ephrin-Bs bind and activate EphAs and EphBs, respectively, with some exceptions (34). Ephs activate factors that regulate actin cytoskeletal reorganization (20). For example, EphBs promote spine development and increase spine stability following their maturation through members of Rho family of small GTPases (25, 35–37), whereas EphAs induce spine remodeling through several other pathways (38–41). However, the precise mechanisms that enable EphAs to directly affect the actin cytoskeleton and facilitate spine remodeling are not well understood.

Here we show that EphA signaling engages a series of events that promote actin, spine, and synaptic reorganization. We found that EphA signaling elicits rapid activation of the actin filament depolymerizing/severing factor cofilin (22) through the phosphatase slingshot 1 (SSH1) (42) and the upstream activator calcineurin/PP2B (43). Both SSH1 and calcineurin are required for EphA-induced actin filament and spine remodeling. Remarkably, EphA signaling causes an initial phase of spine elongation that is followed by synapse reorganization and ultimately spine retraction. This study uncovers a novel molecular pathway utilized by EphAs to restructure excitatory synaptic connections and reveals the time course for these reorganization events.

EXPERIMENTAL PROCEDURES

Animals—Animal procedures were performed in accordance with the guidelines of the Canadian Council for Animal Care and the Montreal General Hospital Facility Animal Care Committee.

DNA Constructs—Full-length V5-tagged, human Slingshot 1 (SSHwt) and a phosphatase-inactive mutant (C393S; now referred to as SSH(CS)) were cloned into pcDNA3 (44). For Semliki Forest virus (SFV) constructs, SSHwt or SSH(CS) cDNAs were each subcloned 3′ to viral subgenomic promoters in the vector pScaPD containing a viral subgenomic promotor followed by farnesylated enhanced green fluorescent protein (EGFP-f) (38, 45). Control viral plasmid contained EGFP-f only.

Antibodies, Recombinant Proteins, and Inhibitors—A custom rabbit polyclonal antibody was raised against a synthesized peptide containing a sequence of 16 amino acids of SSH1 (KSAPEHLKSPSRVNKS) that covers a partially conserved region in both human and mouse SSH1 but not retained in SSH2 or SSH3. Antibodies for the following proteins were also used: cofilin (Cell Signaling Technology, Beverly, MA), phospho-cofilin (Cell Signaling Technology), GAPDH (Abcam, Cambridge, MA), PSD-95 (BD Biosciences, Franklin Lakes, NJ), synapsin I (Synaptic Systems, Goettingen, Germany), V5 (Sigma), and control mouse IgGs (Jackson Immunochemicals, West Grove, PA). Actin filaments were detected using Alexa 568 phalloidin (Invitrogen). The following recombinant proteins were used: human IgG Fc (Jackson Immunochemicals, West Grove, PA) and ephrin-A3 Fc (R & D Systems, Minneapolis, MN). The calcineurin/PP2B inhibitor FK506 was obtained from Sigma.

Dissociated Neuronal Cultures—Primary hippocampal neurons were cultured from P0 C57/B16 mice on coverslips above an astrocyte feeder layer using a modified method previously published (46–48). Briefly, the hippocampal astrocyte feeder layer was prepared by plating mouse astrocytes 5 days before neuronal dissection in astrocyte medium (minimal essential medium containing Earle's salts and L-glutamine supplemented with 10% horse serum, 0.6% glucose and 1% penicillin/streptomycin) (Invitrogen). 24 h prior to dissection, the medium was replaced with Neurobasal-A™ medium supplemented with 2% B27, 1 mM GlutaMAX™, and 1% penicillin/streptomycin (Invitrogen). Hippocampal neurons were dissociated by papain treatment (0.1% papain, 0.02% BSA in Neurobasal-A™ medium) followed by trituration with a fire-polished glass pipette in Neurobasal-A™ medium containing trypsin inhibitor (1%) (Sigma) and BSA (1%). The neurons were then plated on coverslips and transferred to dishes containing the astrocyte feeder layers after 3 h.

Immunostaining and Analysis of Dissociated Neurons—To visualize dendritic spines, F-actin, and synaptic punctae in primary hippocampal neurons, 13-day-old neurons were infected with Semliki Forest virus expressing EGFP-f only or SSH(CS) and EGFP-f. The next day, neurons were either pretreated with FK506 for 10 min or directly treated with Fc or ephrin-A3 Fc for the times indicated. The neurons were washed with ice-cold PBS and fixed with 4% paraformaldehyde, 0.1 M phosphate buffer, 4% sucrose for 10 min. The cells were permeabilized following fixation in PBS containing 0.2% Triton X-100 and immunolabeled with antibodies in 5% BSA/PBS against PSD-95 (1:100) and synapsin (1:300) as indicated. After three washes in PBS, primary antibodies were revealed with a 1-h incubation with Alexa Fluor secondary antibodies (1:300, 5% BSA/PBS) and confocal microscopy. For visualization of F-actin, Alexa 568 phalloidin (1:50) was added to the secondary antibody incubation step. All of the measurements described below were obtained using ImageJ (National Institutes of Health). For measurement of synaptic punctae, RGB overlays of red (synapsin) and green (PSD-95) images (channels were separately thresholded to exclude background noise) were used. Colocalization masks were generated using the "RG2B colocalization" ImageJ plugin (using default parameters) and then overlaid with EGFP-f images to visualize the dendrites and spines. ImageJ was used to measure dendritic spine density, length, synaptic punctae size, and distance from the dendritic shaft. For measurements of F-actin cluster size, intensity, and circularity,

the images were cropped and thresholded in ImageJ. "Analyze particles" was used to obtain measurements of F-actin punctae size, intensity, and circularity. For measuring fluorescence intensity changes along a spine, a line was drawn across a spine, and the fluorescence intensity of the signal in each channel was measured in ImageJ. The spine head, neck, and dendritic shaft regions were approximated using the EGFP-f label.

Hippocampal Slice Preparation—Organotypic hippocampal slices were prepared as described (38, 49). Briefly, 300-μm slices from postnatal day 5 mouse pups were made using a McIllwain tissue chopper (Stoelting, Kiel, WI) and transferred onto semi-porous tissue culture inserts (0.4-μm pore size; Millipore, Billerica, MA) containing medium (50% minimum essential medium, 25% horse serum, 25% Hanks' balanced salt solution, 6.5 mg/ml D-glucose, 0.5% penicillin/streptomycin, pH ~7.2). The medium was replaced every 2 days, and slices were cultured for 1 week prior to viral gene delivery. 16–20 h post-infection, the slices were fixed and mounted for confocal imaging or subjected to immunofluorescence using anti-V5 antibodies.

Semliki Forest Virus Plasmid Construction and Virus Preparation—For expressing SSH1 constructs and fluorescent proteins in hippocampal slices, SFV constructs were created using established techniques (50, 51). Viral particles were created by cotransfecting SFV vectors (see DNA constructs section for plasmids used) with a viral packaging vector into baby hamster kidney cells (52). 72 h following transfection, the cell medium was removed and purified on a sucrose gradient (20%, 55% w/v) by ultracentrifugation. Viral particles were collected and diluted with PBS and concentrated using a filter column (Millipore) and low speed centrifugation. Viral particles were reconstituted in ice-cold PBS, activated with chymotrypsin (10 mg/ml), and treated with aprotinin (10 mg/ml). SFV particles were injected into hippocampal slices with a Picospritzer (Parker Hannifin, Cleveland, OH) or directly apply to culture medium (for dissociated hippocampal neuronal cultures).

Confocal Imaging and Spine Analysis—Confocal imaging of spine morphology in dissociated hippocampal neurons and slices was performed as previously described using a Nikon Eclipse TE-2000 microscope with either a Plan Fluor 20× (0.45 N.A.) or Plan Fluor 60× (1.25 N.A.) objective connected to a Ultraview Spinning Disc confocal system (38, 47). For imaging in organotypic slices, images of dendrites were taken for each condition (control, SSHwt, or SSH(CS)) from at least three independent experiments. Each image contained a Z-stack maximum projection of a primary apical dendrite from a CA1 pyramidal cell taken ~100 μm from the cell body. All of the images were normalized for EGFP-f signal intensity using Adobe Photoshop. Geometric measurements of spine parameters (total length, head length, head width, neck length, neck width, spine area, spine density) were acquired using the Reconstruct computer program. All spine analysis was performed by an investigator blind to the experimental conditions.

RNAi—The siRNA duplexes composed of 21-bp sense and antisense oligonucleotides were purchased from Qiagen along with Allstars negative control siRNAs. The sequences of siRNA for mouse SSH1 used were GGC UUG UUU GCG UAC CAU ATT and CGU UUA GAU CAC ACC AGU ATT. HT22 cells were transfected with 30 pM SSH1 siRNAs or control siRNAs using HiPerFect (Qiagen), and protein knockdown was determined after 72 h.

Western Blot Analysis—For HT22 cell experiments, the cells (~80% confluency) were serum-starved for 1 h before being stimulated with control Fc or ephrin-A3 Fc (10 μg/ml) for 5 min. The cells were then lysed in radioimmune precipitation assay buffer (1% Triton X-100, 1% sodium deoxycholate, 0.1% SDS, 20 mM Tris, 150 mM NaCl, 1 mM EDTA) containing protease inhibitors and orthovanadate. The lysates were then subjected to Western blot. The degree of cofilin phosphorylation was determined using antibodies against phospho-cofilin. The membranes were then stripped and reprobed for total cofilin levels. For densitometry, the amount of phosphorylation was quantified using ImageJ and was normalized against the total cofilin levels. The data were collected over at least three independent experiments.

For biochemistry experiments involving hippocampal neurons, 14 days *in vitro* (DIV) dissociated hippocampal neurons were treated with control Fc or ephrin-A3 Fc (10 μg/ml) for 5 min and then subjected to Western blot analysis as described above.

Cell Rounding Assays—For cell rounding assays, HT22 cells were transfected in 60-mm dishes as described in the figure legends. For rescue experiments, siRNA transfection occurred 24 h prior to DNA transfection, and DNA transfection was for 48 h in total. The cells were seeded onto chambered slides (Nunc, Rochester, NY) at 24 h post-transfection at a density of 25,000 cells/ml. The following day, the cells were stimulated and fixed with 4% paraformaldehyde, 0.1 M phosphate buffer for 30 min, rinsed with TBS, and incubated for 1 h in blocking solution (5% goat serum, 0.1%Triton X-100 in TBS). The cells were then incubated with Alexa 568 phalloidin (Invitrogen) in blocking solution for 1 h followed by brief washes with TBS, 0.1% Triton X-100 and then mounted for confocal microscopy. Ten images were taken from randomly chosen areas for each condition over three independent experiments. Cell counts (>100/condition) were performed by an investigator blind to the experimental conditions.

SSH1 Localization Analysis—For the analysis of SSH1 localization in neurons, V5-tagged SSHwt was introduced into hippocampal neurons along with EGFP-f for 16 h. The cells were then subjected to immunostaining for the V5 epitope, PSD-95, and/or phalloidin labeling to visualize F-actin as described above.

RESULTS

EphA Signaling Promotes Time-dependent Reorganization of Synapses and Spines—EphA receptors are known to induce dendritic spine retraction in organotypic hippocampal slices and dissociated hippocampal neurons (38, 39, 41, 53). Retraction events have been observed after prolonged (45 min to 4 h) stimulation of EphA receptors with ephrin-A protein but not EphB receptors with ephrin-B protein (53). We were interested in characterizing the temporal dynamics of EphA-mediated spine changes and determining the impact of EphA signaling on reorganization of pre- and postsynaptic components of spines. To investigate this, we activated EphA receptors on hippocam-

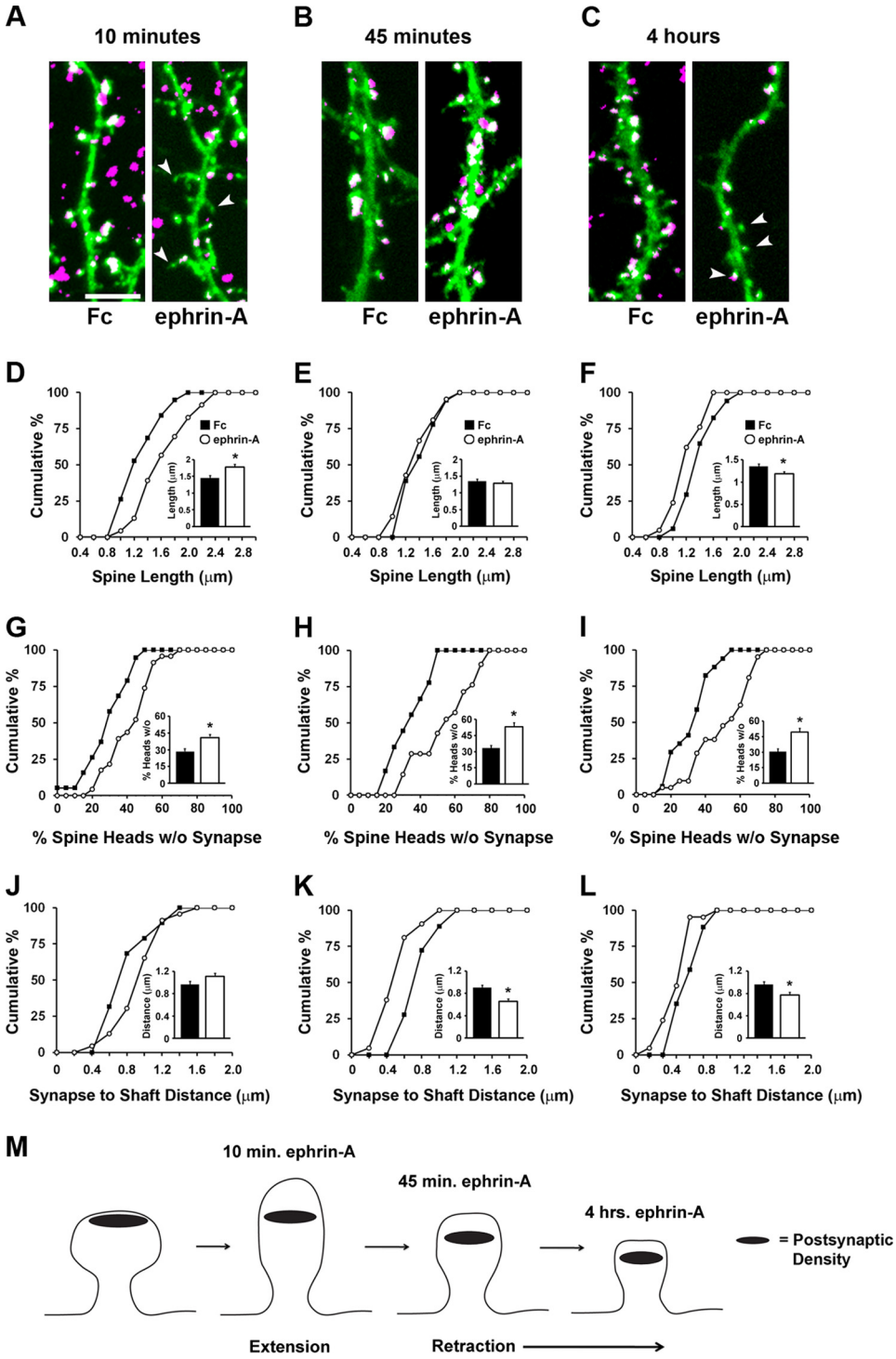

FIGURE 1. **Time-dependent effects on spine morphology and synapses by EphA activation.** *A–L*, hippocampal neurons cultured for 14 DIV and expressing EGFP-f were stimulated with Fc control or ephrin-A for 10 min (*A*, *D*, *G*, and *J*), 45 min (*B*, *E*, *H*, and *K*), and 4 h (*C*, *F*, *I*, and *L*) prior to fixation and staining for synapsin and PSD-95. Shown is EGFP-f to delineate the cell membrane and colabeled punctae of synapsin/PSD-95 to demarcate synapses. *D–I*, cumulative distribution plots and graphs displaying average values of various spine parameters for each stimulus condition and time period. *D*, *, $p = 0.004$, Mann Whitney *U* test. *E*, $p = 0.456$, two-tailed *t* test. *F*, *, $p = 0.037$, two-tailed *t* test. *G*, *, $p = 0.003$, two-tailed *t* test. *H*, *, $p = 0.00015$, two-tailed *t* test. *I*, *, $p = 0.0005$, Mann Whitney *U* test. *J–L*, the effect of ephrin stimulation on the distance of synapses to dendritic shafts following 10 min (*J*), 45 min (*K*), and 4 h (*L*) of EphA stimulation. *J*, $p = 0.687$ Mann Whitney *U* test. *K*, *, $p = 0.002$, Mann Whitney *U* test. *L*, $p = 0.113$, Mann Whitney *U* test. For the 10-min time point, $n = 19$ for Fc control and $n = 23$ for ephrin-A Fc; for the 45 time point, $n = 18$ for Fc control and $n = 21$ for ephrin-A Fc; and for the 4-h time point, $n = 17$ for Fc control and $n = 21$ for ephrin-A Fc. The data were collected from three independent experiments. *M*, schematic showing the time-dependent changes in spines and synapses following EphA activation. *Scale bar*, 5 μm. The *error bars* indicate S.E.

pal neurons grown for 14 DIV and expressing membrane-targeted EGFP-f with ephrin-A Fc or control Fc proteins for 10 min, 45 min, and 4 h. At this stage of culture, many of the synapses on the neurons are mature, and spines are easily observed. Following these treatments, neurons were fixed and labeled for synapsin I, a presynaptic terminal marker, and PSD-

95/SAP90, a marker of the postsynaptic density and whose presence correlates with spine stabilization (54, 55). Surprisingly, we found that after 10 min of ephrin-A treatment, spines showed a significant increase in length (Fig. 1, *A* and *D*). This early spine extension occurred simultaneously with a loss of synapsin I/PSD-95 punctae from the head of spines (Fig. 1*G*). By 45 min, however, the spines had retracted and were similar in average length to those in the Fc treatment condition (Fig. 1, *B* and *E*). Despite this, a large proportion of spine heads lacked synapsin I/PSD-95 punctae (Fig. 1*H*). Furthermore, synaptic punctae were on average closer to the shaft (Fig. 1*K*). By 4 h, spine length became significantly reduced (Fig. 1, *C* and *F*), the percentage of spine heads without synapses remained increased (Fig. 1*I*), synaptic punctae were displaced closer to the dendritic shaft (Fig. 1*L*), and synapse density was significantly reduced (data not shown). Remarkably, EphA activation increased the percentage of synapses formed on dendritic shafts at 45 min and 4 h, without changing the overall density of spines (supplemental Fig. S1). These results indicate that EphA activation results in a series of time-dependent events that modify spines and the location of synaptic components. An early transient phase of spine growth occurs within 10 min of EphA activation and is followed by relocation of synaptic punctae and dendritic spine retraction (depicted in Fig. 1*M*).

EphA Signaling Promotes Rapid Dephosphorylation of Cofilin—Spine retraction through EphAs requires several signaling pathways including those downstream of Cdk5, phospholipase Cγ1, and β1-integrin (38–41). However, the molecular events that underlie the early destabilization of spine morphology after 10 min of EphA activation remain unknown. We previously showed that EphA signaling alters the association of the actin-binding protein cofilin with the cell membrane (38). However, an important question that remained was whether EphA signaling resulted in the activation of cofilin, a potent regulator of actin filament turnover in cells (23, 27, 56). Cofilin activity is tightly regulated by phosphorylation on serine 3 at the N terminus of the protein (27), and cofilin function is required for spine maintenance (25, 26, 57). The degree of serine 3 phosphorylation of cofilin can be probed using antibodies raised against the phosphorylated serine 3 residue. We followed up on the possibility that activation of EphAs with ephrin-A ligands regulates the phosphorylation state of cofilin. We found that stimulation of HT22 cells, an immortalized mouse hippocampal cell line (58), with ephrin-A caused a significant reduction in cofilin phosphorylation after 45 min when compared with control Fc (Fig. 2*A*). We next examined the time course of the dephosphorylation event. Cofilin was dephosphorylated over the course of minutes (2 and 5 min shown; Fig. 2*B*), suggesting rapid dephosphorylation and activation of cofilin in response to EphA activation. To determine whether this signaling event occurred in neurons, we stimulated hippocampal neurons grown for 14 DIV. Similar to the results with HT22 cells, stimulation of neurons with ephrin-A led to a rapid decrease in cofilin phosphorylation (5 min of stimulation; Fig. 2*C*). These results show that stimulation of EphA receptors with ephrin-A causes a rapid decrease in cofilin phosphorylation in both heterologous cells and neurons in culture.

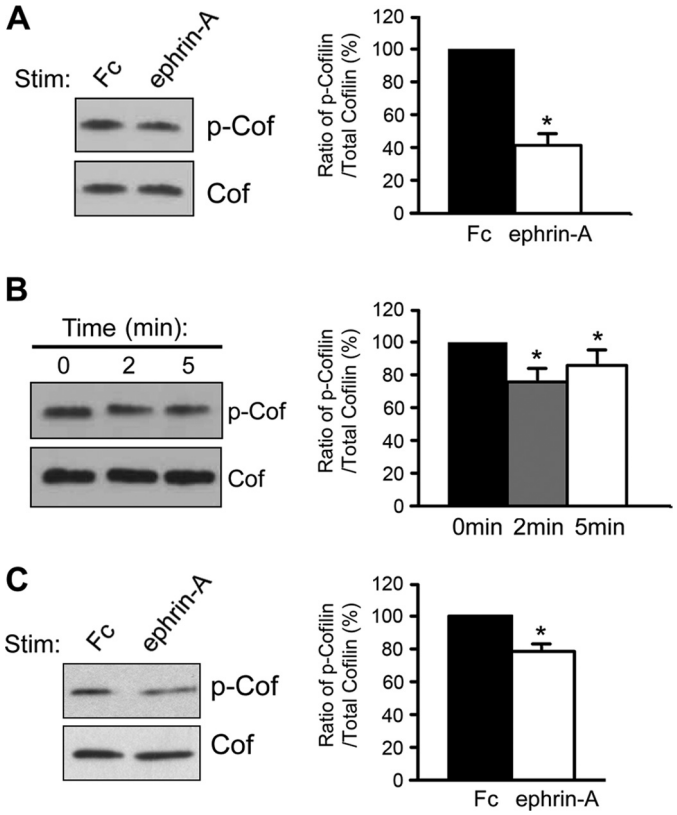

FIGURE 2. **EphA stimulation leads to cofilin dephosphorylation and activation in HT22 cells and hippocampal neurons.** *A*, stimulation of HT22 cells with ephrin-A for 45 min decreased the level of phosphorylated cofilin compared with cells treated with control Fc (*, $p < 0.01$, *t* test, $n = 3$). *B*, cofilin dephosphorylation was observed 2 and 5 min after initiating ephrin-A3-Fc stimulation of HT22 cells (*, $p < 0.05$, one-way ANOVA with Bonferroni test, $n = 3$). *C*, ephrin-A treatment of neurons (14 DIV) for 5 min caused a significant reduction in the level of phospho-cofilin as compared with neurons treated with control Fc (*, $p < 0.05$, unpaired *t* test, $n = 5$). Phospho-cofilin levels were corrected according to total cofilin levels in all graphs. The *error bars* indicate S.E. *Cof*, cofilin; *P-Cof*, phospho-cofilin.

The Cofilin Phosphatase Slingshot 1 (SSH1) Is Required for EphA-mediated Cofilin Dephosphorylation and Cell Morphology Changes—To date, only members of the slingshot and chronophin family of phosphatases have been found to dephosphorylate cofilin on serine 3 and contribute to its direct activation (42, 59–61). Previously it was shown that SSH family members (SSH1, SSH2, and SSH3) are expressed in the adult CNS including the hippocampus (62). Thus, we were interested in investigating whether SSH phosphatases may contribute to cofilin dephosphorylation in response to ephrin-A. To test the requirement of SSH proteins on EphA-mediated cofilin dephosphorylation, we utilized a phosphatase inactive form of SSH1 (SSH(CS)) that harbors a mutation (cysteine 393 replaced by serine in the phosphatase domain) (42). This phosphatase-inactive mutant has been used to interfere with SSH1 activity in cells in several cellular contexts (42, 44, 61). Consistent with other reports, transfection of the SSH(CS) into heterologous cells increased cofilin phosphorylation (supplemental Fig. S2*A*). We next tested the importance of SSH1 function in EphA-mediated cofilin dephosphorylation by treating SSH(CS)-transfected HT22 cells with control Fc or ephrin-A. Expression of SSH(CS) effectively blocked the ability of ephrin-A to cause cofilin dephosphorylation (Fig. 3*A*). Similarly, dissociated neu-

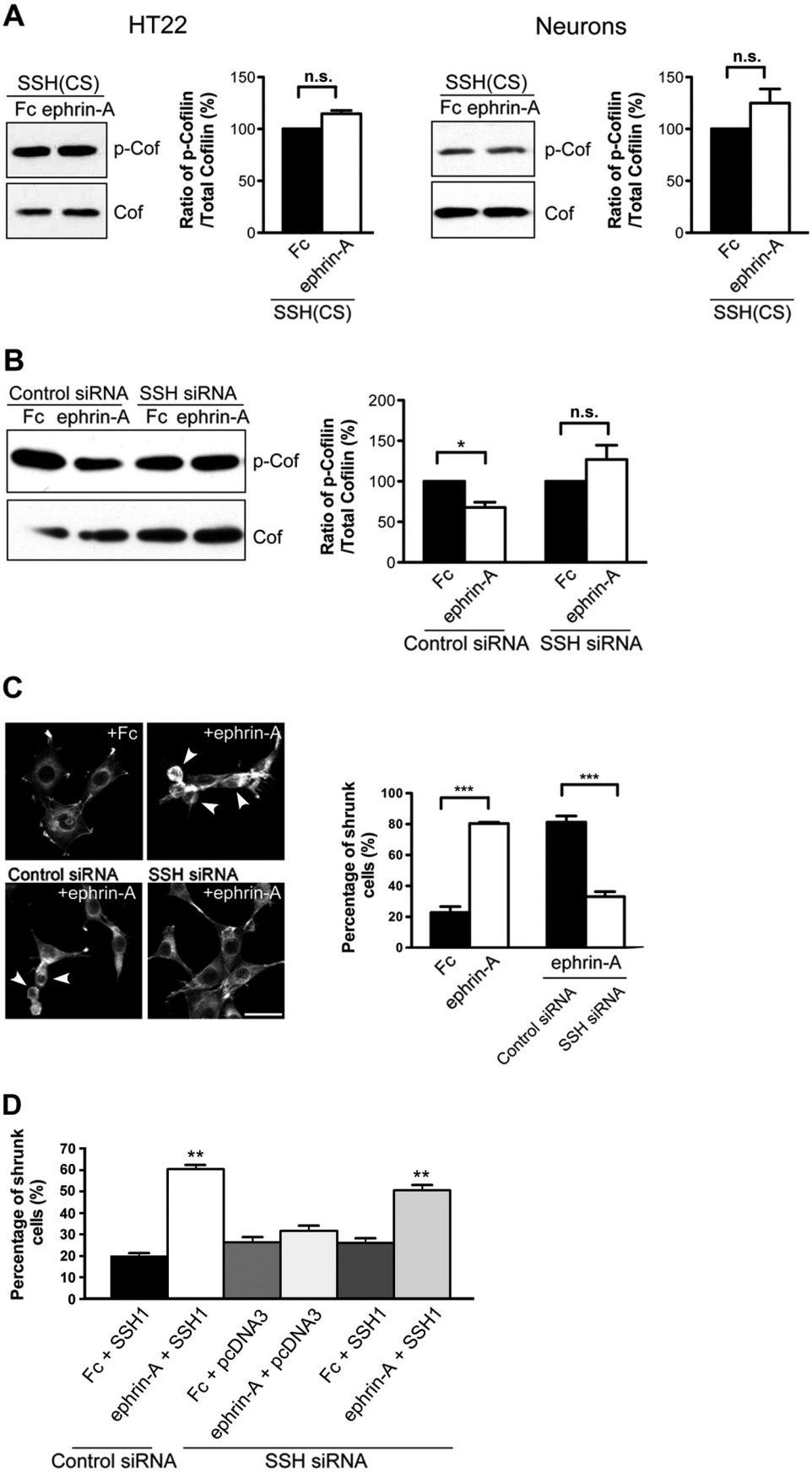
A
HT22
Neurons
SSH(CS)
Fc ephrin-A
p-Cof
Cof
Ratio of p-Cofilin /Total Cofilin (%)
n.s.
Fc
ephrin-A
SSH(CS)
B
Control siRNA
SSH siRNA
Fc ephrin-A Fc ephrin-A
p-Cof
Cof
Ratio of p-Cofilin /Total Cofilin (%)
*
n.s.
Fc
ephrin-A
Control siRNA
SSH siRNA
C
+Fc
+ephrin-A
Control siRNA
SSH siRNA
+ephrin-A
+ephrin-A
Percentage of shrunk cells (%)
***
***
Fc
ephrin-A
ephrin-A
Control siRNA
SSH siRNA
D
Percentage of shrunk cells (%)
**
**
Fc + SSH1
ephrin-A + SSH1
Fc + pcDNA3
ephrin-A + pcDNA3
Fc + SSH1
ephrin-A + SSH1
Control siRNA
SSH siRNA

rons expressing SSH(CS) were unable to reduce cofilin phosphorylation levels upon ephrin-A stimulation (Fig. 3*A*). To test whether SSH(CS) caused an effect similar to that of a direct loss of SSH protein, we reduced endogenous SSH1 in HT22 cells using siRNAs specific for mouse SSH1. Control or SSH1 siRNAs were transfected into HT22 cells, and loss of SSH1 protein was observed 72 h later by Western blot (supplemental Fig. S2, *B* and *C*). Consistent with the effect of the SSH(CS) protein, SSH siRNAs interfered with the ability of ephrin-A stimulation to reduce cofilin phosphorylation levels (Fig. 3*B*). These results show that SSH1 is necessary for the dephosphorylation of cofilin upon EphA activation.

Eph signaling is known to induce rapid actin remodeling and cell rounding in heterologous cells (63–65). HT22 cells also displayed robust actin reorganization and cell rounding upon treatment with ephrin-A. Ephrin-A increased the percentage of cells showing a rounded/shrunken morphology from 22.8% (control levels) to 80.4% following treatment (Fig. 3*C*). We were next interested in determining whether the loss of SSH1 would prevent ephrin-A-induced actin reorganization and cell rounding. To do this, the cells were transfected with either control or SSH1 siRNAs and then stimulated with ephrin-A. We found that ephrin-A treatment caused 81.3% cell rounding in control siRNA-transfected cells. However, this effect was reduced to 33.1% following transfection with SSH1 siRNA (Fig. 3*C*). We verified that the effect of SSH1 siRNA was specific to knockdown of SSH1 by performing rescue experiments using a siRNA-resistant human SSH1. Expression of human SSH was able to restore cell rounding induced by ephrin-A in SSH1 siRNA-transfected cells (Fig. 3*D*). These results, along with those presented earlier, indicate that SSH1 is required for EphA-induced cofilin dephosphorylation, actin remodeling, and cell morphology changes.

SSH1 Is Expressed in Developing and Adult Hippocampus and Is Necessary for Maintaining Dendritic Spine Morphology—Because little is known about the temporal or spatial properties of SSH1 in the hippocampus, we performed a detailed analysis of its expression in neurons to increase our understanding of its role in EphA signaling. We first investigated the temporal expression of SSH1 in the early postnatal and adult hippocampus. Western blot analysis showed that SSH1 protein is detectable at early postnatal time points (P1–P5), prior to being found at a reduced level by P12 and in the adult (Fig. 4*A*). To resolve the subcellular localization of the protein, we turned to dissociated hippocampal cultures where individual neurites and synapses can be resolved more easily. Immunostaining of neurons at 14 DIV for SSH1 showed that the protein was distributed as punctae along the neurites. SSH1 was found in the shafts of dendrites and in spines and showed partial colocalization with PSD-95 (Fig. 4*B*).

To further examine whether SSH1 is enriched at specific subcellular dendritic compartments on hippocampal neurons, we expressed V5-tagged SSH1wt in dissociated hippocampal neurons. The SSH1wt protein was expressed simultaneously with EGFP-f to delineate the dendrites and their spines. Similar to endogenous SSH1 expression, we found that SSH1wt was expressed in dendrites and was enriched in the head of dendritic spines, as shown by colocalization with PSD-95 and F-actin (Fig. 4*C*). Together these findings indicate that SSH1 is found in the dendrites of hippocampal neurons and can be localized in dendritic spines.

Because SSH1 was detected during early postnatal development of the hippocampus, a time when spines are developing, we tested whether SSH1 influences spine morphology. SSHwt or SSH(CS) along with EGFP-f were introduced for 16–20 hours into CA1 pyramidal cells of organotypic hippocampal slices grown for 1 week. Overexpression of SSHwt did not significantly affect the structural properties of spines as compared with control neurons only expressing EGFP-f (Fig. 5). In contrast, the SSH(CS) protein caused a significant distortion of spine morphology, including an increase in spine head length and a reduction in spine head width (Fig. 5, *F* and *G*), without affecting spine density or spine head area. Taking several parameters of the spines in the various conditions into account (including spine length, width, and ratios of these parameters), expression of the SSH(CS) protein in CA1 cells significantly altered the normal morphological distribution of spines. Loss of SSH1 function reduced the percentage of mushroom-shaped spines and increased the percentage of irregular-looking spines with an elongated morphology (Fig. 5). These results demonstrate that SSH1 functions to preserve spine structure.

Calcineurin Is Required for Ephrin-A-induced Cofilin Dephosphorylation and Changes in Cell Morphology—We next sought to delineate further the pathway linking EphA signaling to SSH1 and cofilin. Previous studies have shown that the phosphatase calcineurin/PP2B dephosphorylates SSH1 (66) and is responsible for activating SSH1 in developing and mature neurons (66–68). This is important for actin remodeling in non-neuronal cells (66), guiding growth cones of developing axons (67) and AMPA receptor trafficking at synapses (69). We were interested in determining whether calcineurin was required for EphA-dependent cofilin dephosphorylation and actin reorganization. To test this, we treated HT22 cells and dissociated neurons with the calcineurin inhibitor FK506 for 10 min prior to control Fc or ephrin-A3 Fc application. We found that FK506 blocked ephrin-induced cofilin dephosphorylation in HT22 cells and neurons (Fig. 6*A*). To determine whether calcineurin was required for EphA-mediated cell rounding, we treated HT22 with FK506 prior to eph-

FIGURE 3. **SSH is required for EphA-mediated cofilin dephosphorylation and actin remodeling.** *A*, expression of SSH(CS) blocked ephrin-A-induced cofilin dephosphorylation in HT22 cells and hippocampal neurons (14 DIV; 5 min stimulation, $n = 3$). *B*, knockdown of SSH1 expression with SSH1 siRNAs blocked the ability of ephrin-A to reduce phospho-cofilin levels in HT22 cells (*, $p < 0.05$, one-way ANOVA with Kruskal-Wallis test, $n = 3$). *C*, HT22 cells were treated with Fc or ephrin-A and cell morphology, and F-actin structures were visualized with Alexa 568-conjugated phalloidin. Ephrin-A treatment caused an increase in the number of shrunken cells when compared with Fc treatment (***, $p < 0.001$, *t* test). SSH1 siRNAs reduced the percentage of shrunk cells upon ephrin-A treatment (***, $p < 0.001$, *t* test). $n = 3$ independent experiments (10 images from randomly chosen areas for each condition for each experiment). *Arrowheads* indicate shrunken cells. *D*, expression of a siRNA-resistant form of SSH1 (human SSH1) was able to restore ephrin-A-induced cell rounding. **, $p < 0.05$, ANOVA with *post hoc* Holm-Sidak test, *versus* all other conditions. *Scale bars*, 10 μm. The *error bars* indicate S.E. *Cof*, cofilin; *P-Cof*, phospho-cofilin; *n.s.*, not significant.

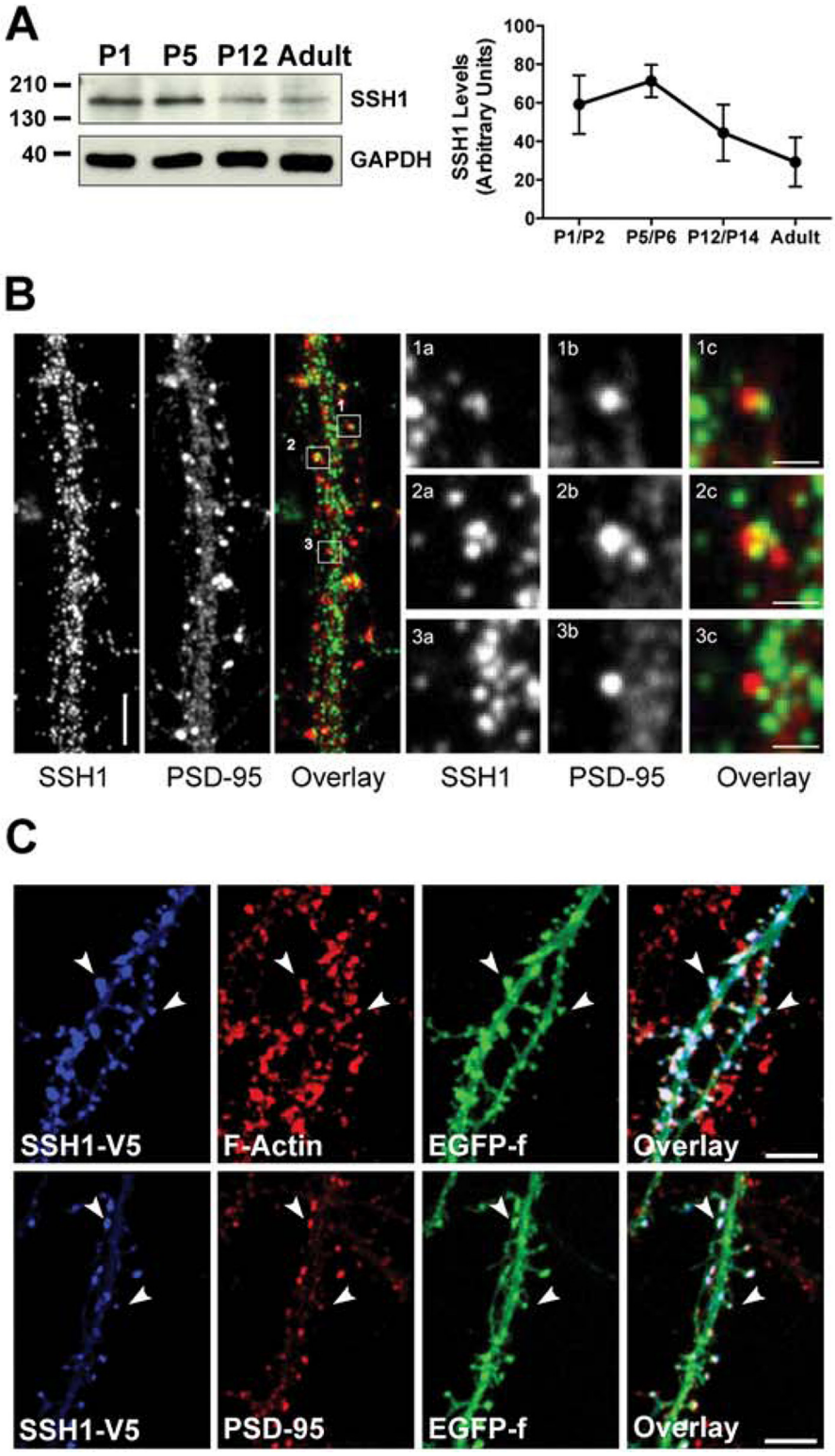

FIGURE 4. **SSH1 is expressed in the developing and adult mouse hippocampus and is localized at dendritic spines.** *A*, Western blot analysis showing that SSH1 protein levels peak during the first postnatal week and decline toward adulthood in mouse hippocampus. *B*, immunostaining of neurons (14 DIV) reveal SSH1 punctae (*green*) localized in neuronal processes, including dendrites and spine heads (*arrows*). *Panels 1a–3c*, SSH1 (*green*) showed partial colocalization with PSD-95 (*red*). *C*, expression of V5-tagged wild type SSH1 (SSHwt) in dissociated hippocampal neurons. SSH1 was concentrated in the head region of the dendritic spines, and immunostaining revealed colocalization with PSD-95 and F-actin (using phalloidin staining). *Scale bars*, 5 μm in *B* and *C* and 1 μm in *panels 1a–3c*. The *error bars* indicate S.E.

rin-A3 Fc treatment and labeled F-actin using Alexa 568 phalloidin. We found that ephrin-induced actin remodeling and cell rounding were significantly blocked by application of FK506 (Fig. 6*B*). These results suggest that calcineurin is required for both EphA-triggered cofilin dephosphorylation and cell rounding.

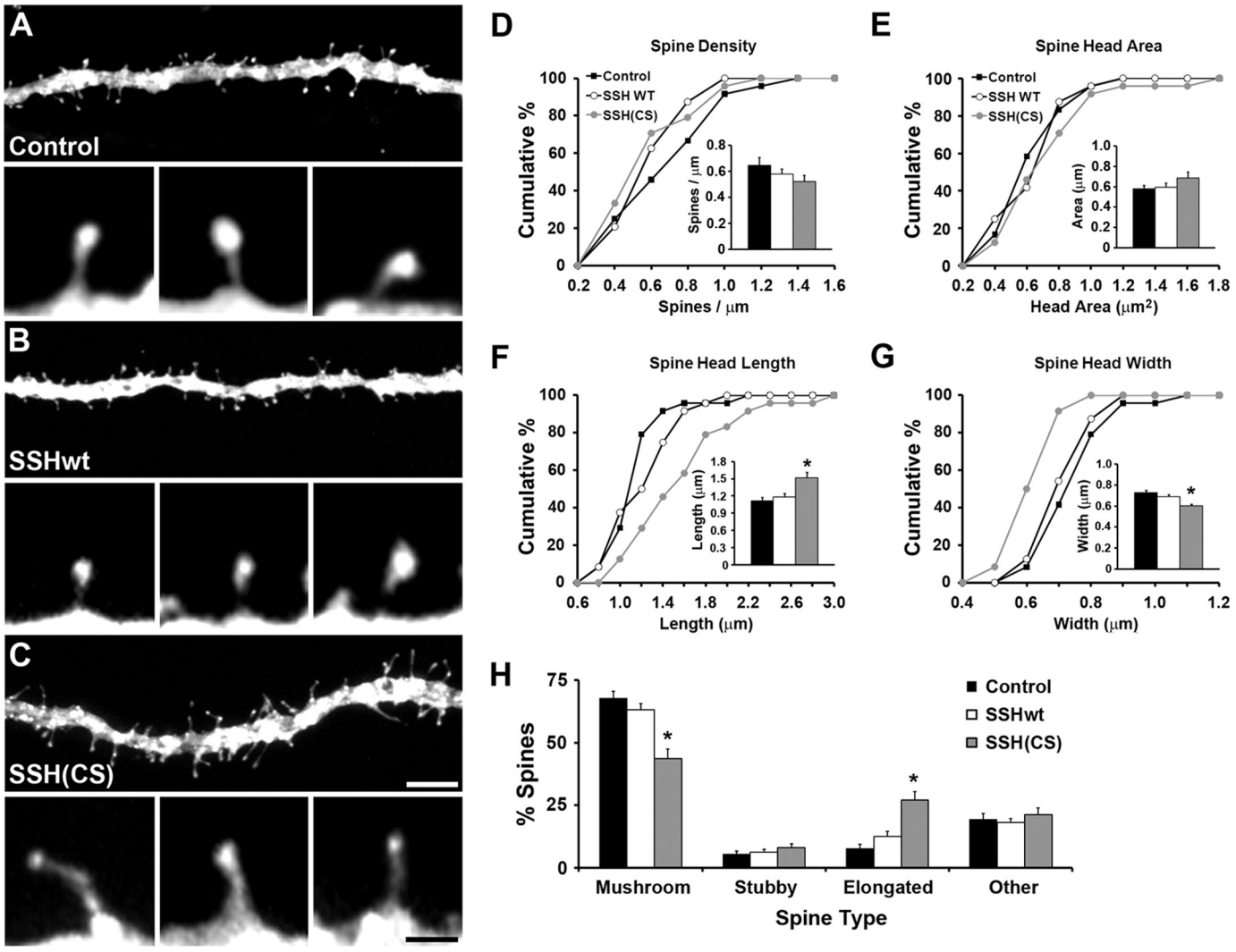

FIGURE 5. **SSH1 is necessary for maintaining CA1 dendritic spine morphology in organotypic hippocampal slices.** *A–C*, examples showing abnormal spine morphology after expression of SSH(CS) when compared with control and SSHwt-expressing CA1 cells. Membrane-targeted EGFP-f was expressed alone (control) or coexpressed with SSHwt or SSH(CS). *D–G*, quantification of spine parameters shows that spine properties were not affected with SSHwt expression. However, spine head length was increased, and spine head width was decreased after expression of SSH(CS). *H*, expression of SSH(CS) decreased the number of mushroom-shaped spines and increased the number of elongated spines (*, $p < 0.05$; **, $p < 0.01$; ANOVA with Student-Newman-Keul's test). $n = 24$ (428 spines total, control), $n = 24$ (419 spines total, SSHwt), and $n = 24$ (410 spines, SSH(CS)) from three independent experiments. *Scale bars*, 5 μm in *A–C* (1 μm in the *insets*). The *error bars* indicate S.E.

SSH1 and Calcineurin Are Required for Early EphA-mediated Spine Extension—We next determined whether SSH1 and calcineurin were required for the rapid changes in spine length caused by EphA signaling. At 13 DIV, neurons were infected with Semliki Forest viruses to drive expression of EGFP-f to reveal spines. The next day, neurons were treated with either control Fc or ephrin-A for 10 min prior to fixation and imaging. Spine density and morphology were compared in each of the conditions. Within 10 min of treating neurons with ephrin-A, the spines showed increased length and decreased head width with no change in density (Fig. 7). Importantly, these modifications to spine morphology were significantly blocked by the presence of the calcineurin inhibitor FK506 or expression of SSH(CS) (Fig. 7). Thus, EphA activation results in a rapid elongation of spines that relies on both calcineurin and SSH function.

EphA Signaling Causes F-actin Reorganization in Spines—To study how early EphA-induced spine remodeling is related to the reorganization of the F-actin network and postsynaptic structure in spines, we investigated the distribution of F-actin in dissociated neurons following ephrin-A treatment and manipulations that block SSH1 and calcineurin function. As shown in Fig. 8*A*, 10 min of ephrin-A application caused spines to elongate, leading to the loss of a well defined head region on spines. Staining for F-actin with Alexa 568 phalloidin revealed that F-actin was redistributed within spines upon ephrin-A treatment from the head region toward the spine neck and dendritic shaft (Fig. 8, *B* and *C*). Furthermore, the ephrin-induced changes in F-actin organization required calcineurin and SSH1 because the redistribution was blocked by application of FK506 or expression of SSH(CS), respectively (Fig. 8, *E* and *G*). To further describe the changes observed in the arrangement of F-actin, we measured several parameters of the F-actin signal in spines. Although overall changes in F-actin cluster size or intensity were not found (Fig. 8, *H* and *I*), the shape of the F-actin clusters in spines was significantly distorted following

EphA activation. This was determined by calculating the degree of circularity of F-actin clusters. Normally, F-actin labeling is detected as round/circular structures enriched in the spine head (70). However, ephrin-A treatment caused a significant elongation of F-actin clusters with a reduced circularity index (Fig. 8*J*). Importantly, application of FK506 or expression of SSH(CS) blocked the reorganization of F-actin by ephrin-A treatment (Fig. 8*J*). These results indicate that ephrin-A treatment reorganizes the F-actin cytoskeleton in spines, and this activity requires the function of SSH1 and calcineurin.

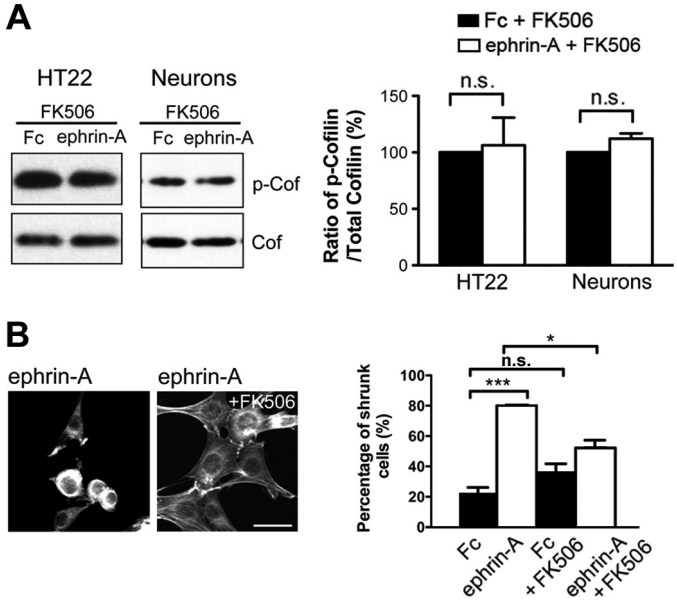

FIGURE 6. **Calcineurin is required for EphA-mediated cofilin dephosphorylation and actin remodeling.** *A*, HT22 cells or neurons were pretreated with the calcineurin inhibitor FK506 (10 mM) for 10 min and then treated with Fc or ephrin-A for 5 min. FK506 blocked the ability of ephrin-A to reduce cofilin phosphorylation ($p > 0.05$, *t* test, $n = 3$). *B*, FK506 significantly reduced the percentage of shrunk cells upon ephrin-A treatment (*, $p < 0.05$; ***, $p < 0.01$; one-way ANOVA with Bonferroni test). $n = 3$ independent experiments (10 images from randomly chosen areas for each condition for each experiment). *Scale bars*, 10 μm. The *error bars* indicate S.E. *Cof*, cofilin; *P-Cof*, phospho-cofilin; *n.s.*, not significant.

DISCUSSION

Eph receptors have an established role in the morphogenesis and maintenance of various tissues (34) and are important regulators of dendritic spines (20, 33). However, the precise mechanisms that allow Eph receptors to perform these functions remain to be fully demonstrated. Our results reveal several novel aspects of EphA signaling and its relationship to spine structural plasticity and synaptic reorganization. First, we show that EphA activation engages a time-dependent series of changes in dendritic spines. EphA signaling initially causes a transient phase of spine elongation. This is accompanied by synaptic relocalization and ultimately spine retraction. Second, we reveal that EphA activation causes the rapid dephosphorylation of cofilin, an important actin filament severing/depolymerizing factor implicated in regulating spine development and morphology. Third, we identify that EphA-induced cofilin activation requires the phosphatases SSH1 and calcineurin. Both phosphatases are needed for EphA-mediated redistribution of actin filaments and spine/synapse remodeling. This study contributes new insight into intricate signaling mechanisms downstream of EphAs that regulate actin-based cellular remodeling and the structural plasticity of excitatory synapses in the central nervous system.

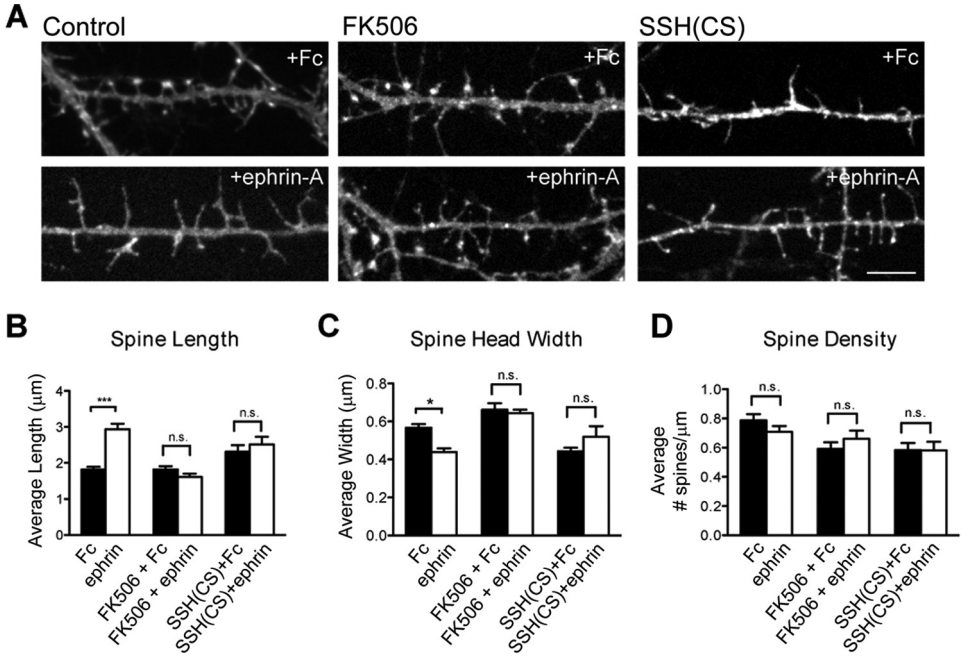

FIGURE 7. **EphA regulation of dendritic spine morphology requires SSH1 and calcineurin.** *A*, examples showing spine morphology after 10 min Fc or ephrin-A treatment. Neurons were infected with SFV expressing EGFP-f to delineate spine morphology or EGFP-f and SSH(CS) to disrupt endogenous SSH1 function. *B* and *C*, ephrin-A treatment caused an increase in spine length and a reduction in spine head width (***, $p < 0.001$; **, $p < 0.01$; one-way ANOVA with Bonferroni test). The presence of FK506 or expression of SSH(CS) abolished ephrin-A-induced spine changes. *D*, spine density was not significantly affected in any group. $n = 15$ for Fc control, $n = 15$ for ephrin-A, $n = 15$ for Fc + FK506, $n = 15$ for ephrin-A + FK506, $n = 15$ for Fc + SSH(CS), and $n = 15$ for ephrin-A + SSH(CS). *Scale bar*, 5 μm. The *error bars* indicate S.E.

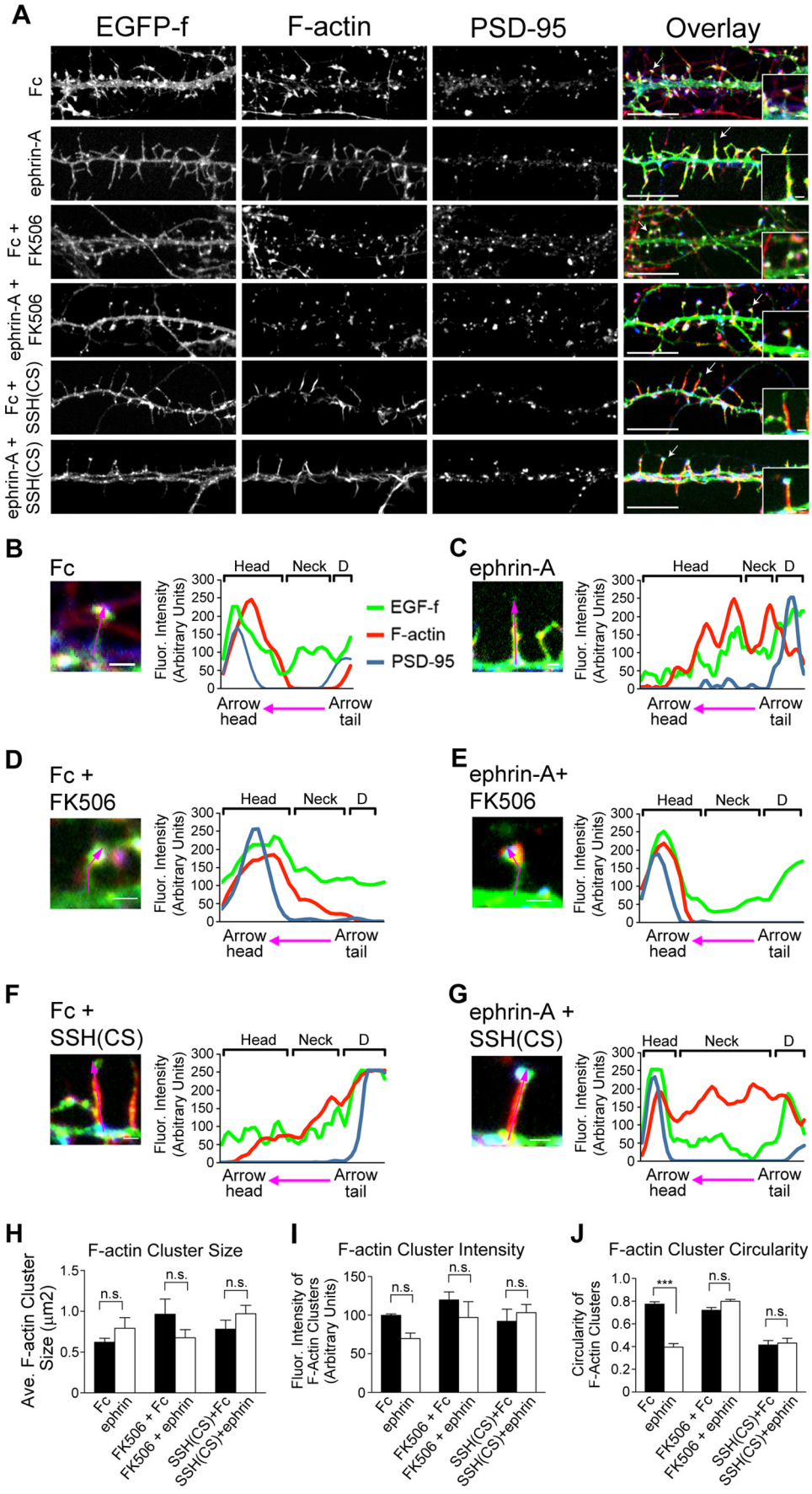
A
EGFP-f
F-actin
PSD-95
Overlay
Fc
ephrin-A
Fc + FK506
ephrin-A + FK506
Fc + SSH(CS)
ephrin-A + SSH(CS)
B
Fc
C
ephrin-A
D
Fc + FK506
E
ephrin-A+ FK506
F
Fc + SSH(CS)
G
ephrin-A + SSH(CS)
Head
Neck
D
Fluor. Intensity (Arbitrary Units)
Arrow head
Arrow tail
EGF-f
F-actin
PSD-95
H
F-actin Cluster Size
Ave. F-actin Cluster Size (μm2)
I
F-actin Cluster Intensity
Fluor. Intensity of F-Actin Clusters (Arbitrary Units)
J
F-actin Cluster Circularity
Circularity of F-Actin Clusters
n.s.
***
Fc
ephrin
FK506 + Fc
FK506 + ephrin
SSH(CS)+Fc
SSH(CS)+ephrin

Early work by Matus (15) showed the importance of actin filament dynamics in spine plasticity. Actin filaments serve as the primary structural scaffold of spines and provide a core for the assembly of protein complexes at synapses. Recent studies have revealed that actin remodeling and spine rearrangements are related to changes in synaptic efficacy (1). The key to spine changes is the recruitment of signaling proteins that refine the actin cytoskeletal network. Indeed, molecules that nucleate, sever, depolymerize, and cap actin filaments regulate spine development and maintenance (18, 20, 26, 71–74). Thus, an elaborate network of actin filament regulatory proteins is available to control the structural plasticity of spines.

Our results indicate that EphAs signal to cofilin to elicit changes in actin distribution in neurons. Cofilin plays a central role in organizing actin filaments in many cell types and is implicated in regulating the development and morphological plasticity of spines (24–26, 56, 57). Cofilin-mediated actin dynamics also affects glutamate receptor trafficking during synaptic plasticity (30). Direct manipulation of cofilin function perturbs spinogenesis and the maintenance of spines (25, 26). In mature hippocampal neurons, expressing a constitutively active form of cofilin results in the formation of longer, immature-looking spines (25). Our results are consistent with this finding, suggesting that activation of cofilin by EphAs promotes actin filament reorganization that results in a time-dependent restructuring of spines. The findings presented here combined with the results from our previous work also suggest that EphA signaling enhances cofilin function on two levels: through decreasing cofilin phosphorylation and thus promoting its activation and reducing its association with the cell membrane (38).

Surprisingly, we found that EphA activation caused an initial phase of spine elongation that was followed by a period of spine retraction. Alterations in actin filament dynamics are likely responsible for this series of spine modifications. Under steady-state conditions in spines, the majority of actin subunits are continuously cycling between an F-actin and G-actin state, with G-actin monomers being added to the barbed ends of actin filaments and dissociated from pointed ends (11, 18). Initial activation of cofilin by EphAs may help sever F-actin in the spine and provide more barbed ends for actin polymerization and transient spine extension. The adjustment to the spine cytoskeleton is accompanied by the loss of PSD-95 clusters from the spine head that may help generate a destabilized or dynamic state of the spine (54, 55). However, prolonged activation of cofilin by EphAs may increase the rate of actin filament disassembly through actin monomer dissociation from both barbed and pointed ends of actin filaments to promote spine retraction (75). Intriguingly, we found a repositioning of synapses closer to dendritic shafts and an accumulation of shaft synapses between 45 min and 4 h of EphA activation. The increase in dendritic shaft synapses may be a consequence of retraction and collapse of some spines while preserving presynaptic inputs (76). EphA signaling likely coordinates the activation of multiple pathways to facilitate these processes. Alteration of β1 integrin signaling by EphA interactions with p130CAS and SPAR may help detach spines from the extracellular matrix to encourage spine retraction/collapse (39, 40). Furthermore, EphA activation of ephexin, a guanine nucleotide exchange factor for Rho family GTPases, may promote actin filament rearrangements and morphological changes in spines by activating RhoA and inhibiting Cdc42 and Rac1 (77). Indeed, EphA signaling through a Cdk5-ephexin complex (41), as well as other signaling intermediates such as phospholipase Cγ1 (38), promotes spine retraction. However, it remains possible that EphA signaling produces additional signaling events that support shaft synapse formation as has been reported for ephrin-B signaling (78).

Interestingly, a recent investigation revealed an opposite role of EphB receptors in increasing cofilin phosphorylation and stabilizing mature spines (25). EphB signaling through the focal adhesion kinase and the RhoA GTPase pathway decreases cofilin phosphorylation and stabilizes spine morphology. Thus, cofilin activity in spines may be finely adjusted by counteracting EphA and EphB signaling. Further experiments are needed to determine the cross-talk between the EphA and EphB signaling systems and the possibility of their coordinated role in regulating spine plasticity through cofilin.

Our study uncovers a novel role for SSH1 in EphA-mediated cofilin activation and spine remodeling. SSH1 can directly bind F-actin (42, 79) and appears to have multiple functions at the synapse. A recent study found that blocking SSH function reduces surface AMPA receptors and synaptic efficacy, as well as impairs the ability of cortical synapses to undergo chemical LTP (69). A plausible role for SSH1 downstream of EphA may be to regulate F-actin levels near the spine neck, a region of the spine that is critical for activity-dependent spine plasticity (17). Indeed, we found that F-actin is accumulated in the neck region of spines by blocking SSH1 function. SSH1 is regulated by several upstream players including the phosphatase calcineurin. Calcineurin activates SSH1 through dephosphorylation, and this pathway facilitates growth cone remodeling during development (67) and AMPA receptor turnover in GABAergic interneurons (68). The ability of cofilin function to be bi-directionally modified by SSH1 and LimK activity to alter the properties of spines (27–29) supports an important and adaptable role of cofilin in synaptic plasticity.

Our findings show that EphA signaling modifies the organization of spines and synapses through a time-dependent pro-

FIGURE 8. **EphA-induced reorganization of postsynaptic F-actin requires calcineurin and SSH1.** *A*, examples of dendrite segments from 14 DIV neurons treated with either Fc or ephrin-A in control conditions or in the presence of FK506 or following SSH(CS) expression. Neurons were stained with Alexa 568-conjugated phalloidin (*red*) and PSD-95 antibody (in *blue*) to visualize F-actin and postsynaptic structures in spines. All of the neurons were expressing EGFP-f to outline dendrite and spine morphology. *B–G*, F-actin distribution across the spine head, neck, and dendritic shaft region following Fc or ephrin-A treatment and with FK506 application or expression of SSH(CS). The plots shown to the *right* of each image show fluorescence intensity changes for F-actin, PSD-95, and EGFP-f along the *magenta line* laid over spines. *Brackets* labeled *D* indicate the dendritic shafts. *H–J*, quantitative analysis of F-actin cluster size, intensity, and circularity. F-actin cluster size and intensity were similar in all conditions ($p > 0.05$, Kruskal-Wallis). However, ephrin-A treatment decreased F-actin cluster circularity (*, $p < 0.05$, Kruskal-Wallis with Dunn's post test). Expression of SSH(CS) alone also significantly changed F-actin cluster circularity (*, $p < 0.05$, Kruskal-Wallis test with Dunn's post test). $n = 6$ (469 particles were analyzed from six dendritic segments across three independent experiments). *Scale bars*, 5 and 1 μm in *insets* and *B–G*, respectively. The *error bars* indicate S.E.

cess involving calcineurin, SSH1, and cofilin. Future studies will investigate the interplay between this EphA pathway and activity-dependent processes that serve to refine excitatory synaptic connections.

Acknowledgment—We thank Dr. A. Fournier (McGill University) for SSH1 constructs.

REFERENCES

1. Kasai, H., Fukuda, M., Watanabe, S., Hayashi-Takagi, A., and Noguchi, J. (2010) Structural dynamics of dendritic spines in memory and cognition. *Trends Neurosci.* **33,** 121–129
2. Yoshihara, Y., De Roo, M., and Muller, D. (2009) Dendritic spine formation and stabilization. *Curr. Opin. Neurobiol.* **19,** 146–153
3. Grutzendler, J., Kasthuri, N., and Gan, W. B. (2002) Long-term dendritic spine stability in the adult cortex. *Nature* **420,** 812–816
4. Trachtenberg, J. T., Chen, B. E., Knott, G. W., Feng, G., Sanes, J. R., Welker, E., and Svoboda, K. (2002) Long-term *in vivo* imaging of experience-dependent synaptic plasticity in adult cortex. *Nature* **420,** 788–794
5. Xu, T., Yu, X., Perlik, A. J., Tobin, W. F., Zweig, J. A., Tennant, K., Jones, T., and Zuo, Y. (2009) Rapid formation and selective stabilization of synapses for enduring motor memories. *Nature* **462,** 915–919
6. Yang, G., Pan, F., and Gan, W. B. (2009) Stably maintained dendritic spines are associated with lifelong memories. *Nature* **462,** 920–924
7. Eaton, B. A., and Davis, G. W. (2003) Synapse disassembly. *Genes Dev.* **17,** 2075–2082
8. Fiala, J. C., Spacek, J., and Harris, K. M. (2002) Dendritic spine pathology. Cause or consequence of neurological disorders? *Brain Res. Brain Res. Rev.* **39,** 29–54
9. Penzes, P., Cahill, M. E., Jones, K. A., VanLeeuwen, J. E., and Woolfrey, K. M. (2011) Dendritic spine pathology in neuropsychiatric disorders. *Nat. Neurosci.* **14,** 285–293
10. Sheng, M., and Hoogenraad, C. C. (2007) The postsynaptic architecture of excitatory synapses. A more quantitative view. *Annu. Rev. Biochem.* **76,** 823–847
11. Okamoto, K., Nagai, T., Miyawaki, A., and Hayashi, Y. (2004) Rapid and persistent modulation of actin dynamics regulates postsynaptic reorganization underlying bidirectional plasticity. *Nat. Neurosci.* **7,** 1104–1112
12. Matsuzaki, M., Honkura, N., Ellis-Davies, G. C., and Kasai, H. (2004) Structural basis of long-term potentiation in single dendritic spines. *Nature* **429,** 761–766
13. Govindarajan, A., Israely, I., Huang, S. Y., and Tonegawa, S. (2011) The dendritic branch is the preferred integrative unit for protein synthesis-dependent LTP. *Neuron* **69,** 132–146
14. Roberts, T. F., Tschida, K. A., Klein, M. E., and Mooney, R. (2010) Rapid spine stabilization and synaptic enhancement at the onset of behavioural learning. *Nature* **463,** 948–952
15. Matus, A. (2000) Actin-based plasticity in dendritic spines. *Science* **290,** 754–758
16. Hotulainen, P., and Hoogenraad, C. C. (2010) Actin in dendritic spines. Connecting dynamics to function. *J. Cell Biol.* **189,** 619–629
17. Honkura, N., Matsuzaki, M., Noguchi, J., Ellis-Davies, G. C., and Kasai, H. (2008) The subspine organization of actin fibers regulates the structure and plasticity of dendritic spines. *Neuron* **57,** 719–729
18. Star, E. N., Kwiatkowski, D. J., and Murthy, V. N. (2002) Rapid turnover of actin in dendritic spines and its regulation by activity. *Nat. Neurosci.* **5,** 239–246
19. Fukazawa, Y., Saitoh, Y., Ozawa, F., Ohta, Y., Mizuno, K., and Inokuchi, K. (2003) Hippocampal LTP is accompanied by enhanced F-actin content within the dendritic spine that is essential for late LTP maintenance in vivo. *Neuron* **38,** 447–460
20. Ethell, I. M., and Pasquale, E. B. (2005) Molecular mechanisms of dendritic spine development and remodeling. *Prog. Neurobiol.* **75,** 161–205
21. Kim, C. H., and Lisman, J. E. (1999) A role of actin filament in synaptic transmission and long-term potentiation. *J. Neurosci.* **19,** 4314–4324
22. Bamburg, J. R. (1999) Proteins of the ADF/cofilin family. Essential regulators of actin dynamics. *Annu. Rev. Cell Dev. Biol.* **15,** 185–230
23. Racz, B., and Weinberg, R. J. (2006) Spatial organization of cofilin in dendritic spines. *Neuroscience* **138,** 447–456
24. Zhou, Q., Homma, K. J., and Poo, M. M. (2004) Shrinkage of dendritic spines associated with long-term depression of hippocampal synapses. *Neuron* **44,** 749–757
25. Shi, Y., Pontrello, C. G., DeFea, K. A., Reichardt, L. F., and Ethell, I. M. (2009) Focal adhesion kinase acts downstream of EphB receptors to maintain mature dendritic spines by regulating cofilin activity. *J. Neurosci.* **29,** 8129–8142
26. Hotulainen, P., Llano, O., Smirnov, S., Tanhuanpää, K., Faix, J., Rivera, C., and Lappalainen, P. (2009) Defining mechanisms of actin polymerization and depolymerization during dendritic spine morphogenesis. *J. Cell Biol.* **185,** 323–339
27. Bernstein, B. W., and Bamburg, J. R. (2010) ADF/cofilin. A functional node in cell biology. *Trends Cell Biol.* **20,** 187–195
28. Meng, Y., Zhang, Y., Tregoubov, V., Janus, C., Cruz, L., Jackson, M., Lu, W. Y., MacDonald, J. F., Wang, J. Y., Falls, D. L., and Jia, Z. (2002) Abnormal spine morphology and enhanced LTP in LIMK-1 knockout mice. *Neuron* **35,** 121–133
29. Schratt, G. M., Tuebing, F., Nigh, E. A., Kane, C. G., Sabatini, M. E., Kiebler, M., and Greenberg, M. E. (2006) A brain-specific microRNA regulates dendritic spine development. *Nature* **439,** 283–289
30. Gu, J., Lee, C. W., Fan, Y., Komlos, D., Tang, X., Sun, C., Yu, K., Hartzell, H. C., Chen, G., Bamburg, J. R., and Zheng, J. Q. (2010) ADF/cofilin-mediated actin dynamics regulate AMPA receptor trafficking during synaptic plasticity. *Nat. Neurosci.* **13,** 1208–1215
31. Klein, R. (2009) Bidirectional modulation of synaptic functions by Eph/ephrin signaling. *Nat. Neurosci.* **12,** 15–20
32. Murai, K. K., and Pasquale, E. B. (2004) Eph receptors, ephrins, and synaptic function. *Neuroscientist* **10,** 304–314
33. Lai, K. O., and Ip, N. Y. (2009) Synapse development and plasticity. Roles of ephrin/Eph receptor signaling. *Curr. Opin. Neurobiol.* **19,** 275–283
34. Murai, K. K., and Pasquale, E. B. (2003) 'Eph'ective signaling. Forward, reverse and crosstalk. *J. Cell Sci.* **116,** 2823–2832
35. Henkemeyer, M., Itkis, O. S., Ngo, M., Hickmott, P. W., and Ethell, I. M. (2003) Multiple EphB receptor tyrosine kinases shape dendritic spines in the hippocampus. *J. Cell Biol.* **163,** 1313–1326
36. Kayser, M. S., Nolt, M. J., and Dalva, M. B. (2008) EphB receptors couple dendritic filopodia motility to synapse formation. *Neuron* **59,** 56–69
37. Moeller, M. L., Shi, Y., Reichardt, L. F., and Ethell, I. M. (2006) EphB receptors regulate dendritic spine morphogenesis through the recruitment/phosphorylation of focal adhesion kinase and RhoA activation. *J. Biol. Chem.* **281,** 1587–1598
38. Zhou, L., Martinez, S. J., Haber, M., Jones, E. V., Bouvier, D., Doucet, G., Corera, A. T., Fon, E. A., Zisch, A. H., and Murai, K. K. (2007) EphA4 signaling regulates phospholipase Cgamma1 activation, cofilin membrane association, and dendritic spine morphology. *J. Neurosci.* **27,** 5127–5138
39. Bourgin, C., Murai, K. K., Richter, M., and Pasquale, E. B. (2007) The EphA4 receptor regulates dendritic spine remodeling by affecting beta1-integrin signaling pathways. *J. Cell Biol.* **178,** 1295–1307
40. Richter, M., Murai, K. K., Bourgin, C., Pak, D. T., and Pasquale, E. B. (2007) The EphA4 receptor regulates neuronal morphology through SPAR-mediated inactivation of Rap GTPases. *J. Neurosci.* **27,** 14205–14215
41. Fu, W. Y., Chen, Y., Sahin, M., Zhao, X. S., Shi, L., Bikoff, J. B., Lai, K. O., Yung, W. H., Fu, A. K., Greenberg, M. E., and Ip, N. Y. (2007) Cdk5 regulates EphA4-mediated dendritic spine retraction through an ephexin1-dependent mechanism. *Nat. Neurosci.* **10,** 67–76
42. Niwa, R., Nagata-Ohashi, K., Takeichi, M., Mizuno, K., and Uemura, T. (2002) Control of actin reorganization by Slingshot, a family of phosphatases that dephosphorylate ADF/cofilin. *Cell* **108,** 233–246
43. Winder, D. G., and Sweatt, J. D. (2001) Roles of serine/threonine phosphatases in hippocampal synaptic plasticity. *Nat. Rev. Neurosci.* **2,** 461–474
44. Hsieh, S. H., Ferraro, G. B., and Fournier, A. E. (2006) Myelin-associated inhibitors regulate cofilin phosphorylation and neuronal inhibition through LIM kinase and Slingshot phosphatase. *J. Neurosci.* **26,** 1006–1015
45. Lundstrom, K., and Ehrengruber, M. U. (2003) Semliki Forest virus (SFV)

vectors in neurobiology and gene therapy. *Methods Mol. Med.* **76,** 503–523
46. Kaech, S., and Banker, G. (2006) Culturing hippocampal neurons. *Nat. Protoc.* **1,** 2406–2415
47. Jones, E. V., Bernardinelli, Y., Tse, Y. C., Chierzi, S., Wong, T. P., and Murai, K. K. (2011) Astrocytes control glutamate receptor levels at developing synapses through SPARC-beta-integrin interactions. *J. Neurosci.* **31,** 4154–4165
48. Jones, E. V., Cook, D., and Murai, K. K. (2012) A neuron-astrocyte coculture system to investigate astrocyte-secreted factors in mouse neuronal development. *Methods Mol. Biol.* **814,** 341–352
49. Stoppini, L., Buchs, P. A., and Muller, D. (1991) A simple method for organotypic cultures of nervous tissue. *J. Neurosci. Methods* **37,** 173–182
50. Ehrengruber, M. U., Lundstrom, K., Schweitzer, C., Heuss, C., Schlesinger, S., and Gähwiler, B. H. (1999) Recombinant Semliki Forest virus and Sindbis virus efficiently infect neurons in hippocampal slice cultures. *Proc. Natl. Acad. Sci. U.S.A.* **96,** 7041–7046
51. Haber, M., Zhou, L., and Murai, K. K. (2006) Cooperative astrocyte and dendritic spine dynamics at hippocampal excitatory synapses. *J. Neurosci.* **26,** 8881–8891
52. DiCiommo, D. P., and Bremner, R. (1998) Rapid, high level protein production using DNA-based Semliki Forest virus vectors. *J. Biol. Chem.* **273,** 18060–18066
53. Murai, K. K., Nguyen, L. N., Irie, F., Yamaguchi, Y., and Pasquale, E. B. (2003) Control of hippocampal dendritic spine morphology through ephrin-A3/EphA4 signaling. *Nat. Neurosci.* **6,** 153–160
54. Ehrlich, I., Klein, M., Rumpel, S., and Malinow, R. (2007) PSD-95 is required for activity-driven synapse stabilization. *Proc. Natl. Acad. Sci. U.S.A.* **104,** 4176–4181
55. Prange, O., and Murphy, T. H. (2001) Modular transport of postsynaptic density-95 clusters and association with stable spine precursors during early development of cortical neurons. *J. Neurosci.* **21,** 9325–9333
56. Fedulov, V., Rex, C. S., Simmons, D. A., Palmer, L., Gall, C. M., and Lynch, G. (2007) Evidence that long-term potentiation occurs within individual hippocampal synapses during learning. *J. Neurosci.* **27,** 8031–8039
57. Carlisle, H. J., Manzerra, P., Marcora, E., and Kennedy, M. B. (2008) SynGAP regulates steady-state and activity-dependent phosphorylation of cofilin. *J. Neurosci.* **28,** 13673–13683
58. Li, Y., Maher, P., and Schubert, D. (1997) A role for 12-lipoxygenase in nerve cell death caused by glutathione depletion. *Neuron* **19,** 453–463
59. Gohla, A., Birkenfeld, J., and Bokoch, G. M. (2005) Chronophin, a novel HAD-type serine protein phosphatase, regulates cofilin-dependent actin dynamics. *Nat. Cell Biol.* **7,** 21–29
60. Huang, T. Y., Minamide, L. S., Bamburg, J. R., and Bokoch, G. M. (2008) Chronophin mediates an ATP-sensing mechanism for cofilin dephosphorylation and neuronal cofilin-actin rod formation. *Dev. Cell* **15,** 691–703
61. Kurita, S., Watanabe, Y., Gunji, E., Ohashi, K., and Mizuno, K. (2008) Molecular dissection of the mechanisms of substrate recognition and F-actin-mediated activation of cofilin-phosphatase Slingshot-1. *J. Biol. Chem.* **283,** 32542–32552
62. Ohta, Y., Kousaka, K., Nagata-Ohashi, K., Ohashi, K., Muramoto, A., Shima, Y., Niwa, R., Uemura, T., and Mizuno, K. (2003) Differential activities, subcellular distribution and tissue expression patterns of three members of Slingshot family phosphatases that dephosphorylate cofilin. *Genes Cells* **8,** 811–824
63. Lawrenson, I. D., Wimmer-Kleikamp, S. H., Lock, P., Schoenwaelder, S. M., Down, M., Boyd, A. W., Alewood, P. F., and Lackmann, M. (2002) Ephrin-A5 induces rounding, blebbing and de-adhesion of EphA3-expressing 293T and melanoma cells by CrkII and Rho-mediated signalling. *J. Cell Sci.* **115,** 1059–1072
64. Dail, M., Richter, M., Godement, P., and Pasquale, E. B. (2006) Eph receptors inactivate R-Ras through different mechanisms to achieve cell repulsion. *J. Cell Sci.* **119,** 1244–1254
65. Irie, F., Okuno, M., Matsumoto, K., Pasquale, E. B., and Yamaguchi, Y. (2008) Heparan sulfate regulates ephrin-A3/EphA receptor signaling. *Proc. Natl. Acad. Sci. U.S.A.* **105,** 12307–12312
66. Wang, Y., Shibasaki, F., and Mizuno, K. (2005) Calcium signal-induced cofilin dephosphorylation is mediated by Slingshot via calcineurin. *J. Biol. Chem.* **280,** 12683–12689
67. Wen, Z., Han, L., Bamburg, J. R., Shim, S., Ming, G. L., and Zheng, J. Q. (2007) BMP gradients steer nerve growth cones by a balancing act of LIM kinase and Slingshot phosphatase on ADF/cofilin. *J. Cell Biol.* **178,** 107–119
68. Yuen, E. Y., and Yan, Z. (2009) Dopamine D4 receptors regulate AMPA receptor trafficking and glutamatergic transmission in GABAergic interneurons of prefrontal cortex. *J. Neurosci.* **29,** 550–562
69. Yuen, E. Y., Liu, W., Kafri, T., van Praag, H., and Yan, Z. (2010) Regulation of AMPA receptor channels and synaptic plasticity by cofilin phosphatase Slingshot in cortical neurons. *J. Physiol.* **588,** 2361–2371
70. Fischer, M., Kaech, S., Knutti, D., and Matus, A. (1998) Rapid actin-based plasticity in dendritic spines. *Neuron* **20,** 847–854
71. Hering, H., and Sheng, M. (2003) Activity-dependent redistribution and essential role of cortactin in dendritic spine morphogenesis. *J. Neurosci.* **23,** 11759–11769
72. Ackermann, M., and Matus, A. (2003) Activity-induced targeting of profilin and stabilization of dendritic spine morphology. *Nat. Neurosci.* **6,** 1194–1200
73. Wegner, A. M., Nebhan, C. A., Hu, L., Majumdar, D., Meier, K. M., Weaver, A. M., and Webb, D. J. (2008) N-wasp and the Arp2/3 complex are critical regulators of actin in the development of dendritic spines and synapses. *J. Biol. Chem.* **283,** 15912–15920
74. Kim, Y., Sung, J. Y., Ceglia, I., Lee, K. W., Ahn, J. H., Halford, J. M., Kim, A. M., Kwak, S. P., Park, J. B., Ho Ryu, S., Schenck, A., Bardoni, B., Scott, J. D., Nairn, A. C., and Greengard, P. (2006) Phosphorylation of WAVE1 regulates actin polymerization and dendritic spine morphology. *Nature* **442,** 814–817
75. Kueh, H. Y., Brieher, W. M., and Mitchison, T. J. (2008) Dynamic stabilization of actin filaments. *Proc. Natl. Acad. Sci. U.S.A.* **105,** 16531–16536
76. Mateos, J. M., Lüthi, A., Savic, N., Stierli, B., Streit, P., Gähwiler, B. H., and McKinney, R. A. (2007) Synaptic modifications at the CA3-CA1 synapse after chronic AMPA receptor blockade in rat hippocampal slices. *J. Physiol.* **581,** 129–138
77. Shamah, S. M., Lin, M. Z., Goldberg, J. L., Estrach, S., Sahin, M., Hu, L., Bazalakova, M., Neve, R. L., Corfas, G., Debant, A., and Greenberg, M. E. (2001) EphA receptors regulate growth cone dynamics through the novel guanine nucleotide exchange factor ephexin. *Cell* **105,** 233–244
78. Aoto, J., Ting, P., Maghsoodi, B., Xu, N., Henkemeyer, M., and Chen, L. (2007) Postsynaptic ephrinB3 promotes shaft glutamatergic synapse formation. *J. Neurosci.* **27,** 7508–7519
79. Huang, T. Y., DerMardirossian, C., and Bokoch, G. M. (2006) Cofilin phosphatases and regulation of actin dynamics. *Curr. Opin. Cell Biol.* **18,** 26–31